Quantifying neuropeptide-induced organ contractions in *Bombyx mori* using a Python-based analysis tool – InsectMotion.

Matej Medla[1*], Vanda Klöcklerová[1], Emma Buchová[1], Daniel Čižmár[2], Ladislav Roller[1], Dušan Žitňan[1]
[1]Institute of Zoology, Slovak Academy of Sciences, Bratislava, Slovakia
[2]Leibnitz Institute for ZOO and Wildlife Research, Department of Reproduction Management, Berlin, Germany

*Corresponding author: matej.medla@savba.sk

ABSTRACT

InsectMotion is a Python-based software tool designed for the post hoc analysis of video recordings that capture movements or muscle contractions in insects and other invertebrates. It provides a simple, fast and automated approach for semi-quantitative assessment of motion by measuring the "pixel activity" expressed by changes in pixel intensity or color. Unlike many existing approaches, it does not require specialized equipment, chemical reagents, or expensive software. The application distinguishes active and inactive pixels within selected regions of interest (ROI) and measure their changing activity over a pre-set time. InsectMotion offers two analysis modes: Graphical Analysis (GA), and Pixel Activity Analysis (PAA), both adaptable to various experiments. GA generates a graphical illustration of pixel activity (in selected ROIs) over time together with numerical data from the measurement. PAA produces binary Portable Network Graphic (PNG) images highlighting the active clusters of pixels in the video. As a follow-up to Čižmár et al. (2019), which identified calcitonin-like diuretic hormone (CT-DH) and myoinhibitory peptides (MIPs) as regulators of male accessory glands and gonoducts in *Bombyx mori*, we used InsectMotion to quantify neuropeptide-induced contractions in multiple silkworm organs. Developed and validated in *B. mori*, InsectMotion also performs reliably in other small arthropods, demonstrating broad applicability for quantitative motion analysis. By lowering the technical barrier for contraction-based assays, InsectMotion supports more accessible phenotypic studies in neurobiology and physiology.

Keywords: *Bombyx mori*, neuropeptides, video analysis, muscle contractions, Insects, Python

INTRODUCTION

Arthropods are the most abundant and diverse group of organisms on Earth, playing major roles in the ecosystem, ranging from commensals to parasitic species. It is important to understand their physiology for developing strategies that will either ensure their protection or mitigate the transmission of pathogen-causing diseases. Most studies are focused on biological functions such as feeding, growth, ecdysis, reproduction, locomotion, and behavior. These studies generally involve physiological or behavioral assays in which outcomes are recorded on video to monitor activity and compare control and test groups. However, post-experimental analysis of such recordings can be labor-intensive and is often limited to qualitative observations or general descriptions.

Physiological transitions in insects and other arthropods are under intense regulation by signaling molecules, such as hormones and neuropeptides, which drive the contraction or relaxation of tissues involved in feeding, excretion, ecdysis, and reproduction (LaJeunesse et al., 2010; Daubnerová et al., 2021; Žitňan et al., 2007). Several neuropeptide families have been identified as regulators of visceral muscle activity in multiple insect species, including MIPs, FMRFamide-related peptides, and CT-DH, further emphasizing the conserved roles of these neuropeptides in arthropod physiology (Matsumoto et al., 2019; Coast et al., 2001; Zandawala, 2012; TeBrugge et al., 2008; Čižmár et al., 2019; Kim et al., 2006). Quantitative and objective measurement of movement or muscle activity are often essential, especially when subtle physiological changes occur during development or in response to neuropeptides and hormonal cues.

Muscle activity in arthropods is most commonly quantified using electromyography (EMG), a technique that was established in insects in the mid-20th century. EMG yields highly quantitative electrical outputs of muscle activity and is widely applied across many model species (Yoshida et al., 2023; Hermanson and Altenbach, 1981; Vo-Doan et al., 2022; Pflüger et al., 2011). However, EMG does not provide a direct visual representation of muscle contractions, requires invasive electrode placement, and often involves specialized equipment and substantial processing pipelines. With these limitations in mind, there is a growing interest in computational approaches for movement quantification.

To fill in this methodological gap, we created InsectMotion, a simple, widely accessible, post-experimental video-based tool specifically designed to detect and quantify, both in time and space, the muscle contractions and fine physiological movements of insects and other arthropods. The tool performs its analysis on "pixel activity" by transforming videos into grayscale and determining pixels whose intensity varies over time. These “active pixels” mark contraction-related motion, while static background pixels do not change in intensity over time. InsectMotion performs two complementary types of analyses: (i) GA, which provides quantification of contraction intensity in time in selected ROIs, and (ii) PAA for the whole-frame visualization of the movement pattern. An extended version, InsectMotion_ext, includes a modified PAA, coloring active pixels red, which significantly enhances visual appearance, in particular for large-scale motions. Both versions are open source and are freely available via GitHub.

This study also directly builds on the findings of Čižmár et al. (2019), who showed that CT-DH and MIPs regulate muscle activity in the male gonoducts of *B. mori*. Because neuropeptides identified in gonoducts frequently co-occur in other visceral tissues, we first used immunohistochemistry to examine the hindgut innervation and confirmed the presence of neuropeptide-expressing neurons both in adult and in the pharate larval stage. Guided by the observed patterns, we extended the functional analysis to these tissues. Using InsectMotion, we further tested a homologous calcitonin peptide from *Ixodes ricinus* (calcitonin 34; CT34; Žitňan et al., unpublished results) selected for its amino-acid similarity to *B. mori* CT-DH. Our results show strong stimulatory effects of CT34 and strong inhibitory effects of MIP-1 in all tissues investigated, thereby broadening the recognized scope of neuropeptide-mediated control of peripheral organ contractility in *B. mori*.

Together, InsectMotion and the present dataset highlight the potential of video-based pixel analysis as a sensitive, user-friendly alternative or complement to EMG, suitable for investigating physiological processes across diverse arthropod systems.

MATERIALS AND METHODS

Table 1: List of neuropeptides used in this study.

Name	Organism	Sequence	Reference
CT34	*I. ricinus*	AGGLLDFGLSRGASGAEAAKARLGLKLANDPYGP-NH_2	(Žitňan et al., unpublished results)
CT-DH	*B. mori*	AFDLGLGRGYSGALQAKHLMGLAAANFAGGP-NH_2	Brugge et al., 2008
MIP-1	*B. mori*	AWQDLNSAW-NH_2	Yamanaka et al., 2010

Table 2: List of antibodies used in this study. Abbreviations: Mm – mouse monoclonal; M – mouse; R – rabbit.

Antibody name	Type	Source	Dilution	Reference
MIP (*M. sexta*)	Primary	Mm	1:1000	Kim et al., 2006
CT-DH (*B. mori*)	Primary	R	1:2000	Park et al., 2008
Alexa Fluor® 488	Secondary	R	1:1000	Jackson Immuno Research
Alexa Fluor® 594	Secondary	M	1:1000	Jackson Immuno Research

Experimental animals

All animal experiments were provided by the breeding facility at the Institute of Zoology SAS and carried out in accordance with the Animal Use Protocol approved by the ethical committee of Biomedical Research Centre of Slovak Academy of Sciences and the State Veterinary and Food Administration of the Slovak Republic (facility number SK U CH01016, permit number 3954/19-221 and 292/16-221k).

The N4 strain of *B. mori* (L.) was reared under a 16:8 h light/dark photoperiod at 25°C. Larvae were fed on mulberry leaves. We used feeding and pharate third- and fourth-instar larvae (n=10) and male adults (n=10) for *in vitro* contraction assays. These samples were collected across three independent experimental replicates, with the final number of individuals per stage representing the combined dataset. A wide range of larval and adult stages of both sexes were used for immunohistochemistry. Pharate stages were defined in line with Žitňan et al. (1999; 2002).

I. ricinus ticks (n=10) were kept in tubes in 95% humidity chambers under a 10:14 h light/dark cycle at 22°C. Unfed male ticks were used only in the experiments focused on locomotion analysis.

Immunohistochemical staining

Whole-mount immunohistochemistry was performed according to previously described protocols (Čižmár et al., 2019; Bednár et al., 2017). A list of primary and secondary antibodies used in this study are shown in Table 2. Dissected samples were fixed in 4% paraformaldehyde for 1 h at room temperature, rinsed in PBS with 0.5% Triton X-100, and blocked with normal donkey serum (NDS) or normal goat serum (NGS). Tissues were then incubated with a mixture of primary antibodies for 48 h at 4°C. Following washes in PBS-Triton, bound primary antibodies were detected using secondary antibodies, which were applied for an overnight incubation at 4°C. Samples were washed again in PBS-Triton, briefly rinsed in PBS: glycerol (1:1), and mounted in 100% glycerol. Stained preparations were visualized using a Nikon Eclipse E600 or TCS SPE-II

confocal system (Leica Microsystems, Germany). Image alignment and assembly of composite figures were carried out using Adobe Creative Cloud (Photoshop, Illustrator, and InDesign).

In vitro and *in vivo* functional assays

Silkworms at specific stages were placed on a Petri dish coated with Sylgard 184 elastomer (Dow Corning Corporation, Midland, MI, USA), immobilized with entomology pins and dissected in physiological saline (140 mM NaCl, 5 mM KCl, 5 mM $CaCl_2$, 4 mM $NaHCO_3$, 1 mM $MgCl_2$, 5 mM HEPES, pH 7.2). After dissection, tissues were rinsed 2–3 times and finally incubated in Ringer´s solution (140 mM NaCl, 5 mM KCl, 2 mM $CaCl_2$, 1 mM MgCl, 10 mM HEPES, 5 mM Glucose, pH 7.2) for the entire duration of *in vitro* assay to prevent desiccation.

In vitro contraction assays were conducted on adult males as well as on pharate third- and fourth-instar larvae to evaluate the sensitivity of the InsectMotion tool in detecting treatment-induced changes in muscle activity. For each individual, muscle contractions were recorded under three sequential experimental conditions: (i) a baseline control measurement taken 5 minutes after placement of the silkworm on a Petri dish (control), (ii) a stimulated state, and (iii) an inhibited state.

Muscle stimulation was achieved by applying 1 µM CT34 (*I. ricinus*). Muscle inhibition was induced by treatment with 1 µM MIP-1 (*B. mori*), following the protocol described by Čižmár et al. (2019). Neuropeptides were prepared as dilutions in Ringer's solution. Each treatment was applied in a final volume of 300–500 µl, by replacing the previous volume of Ringer's solution to ensure consistent exposure conditions. Recording began immediately after neuropeptide application, and the duration for all conditions was standardized to 3–5 minutes.

Movement analysis at a larger scale was conducted by monitoring the *in vivo* locomotion of *I. ricinus* ticks. Males were individually placed in regular Petri dishes, and their activity was stimulated using human breath, following the method of Vassallo and Pérez (2002). Recording started immediately after activation and continued for up to 30 seconds.

Video acquisition and analysis

All experiments were monitored under a binocular microscope Leica S9D or Leica M205 C, and photographed and recorded using a camera Leica Flexacam C1 or Leica Flexacam C3, with fixed zoom, focus, and field of view. Illumination was provided by an LED ring light (e.g., Leica LED5000 HDI), and recordings were captured at a resolution of 1280 x 720 pixels and a frame rate of 30 frames per second. Recordings were processed using InsectMotion, which includes two complementary analytical modules. GA was performed on the full 3–5 min recordings to quantify ROI-based contraction dynamics, whereas PAA was conducted on trimmed 30-s segments (using Canva) to optimize processing time during whole-frame activity evaluation. Final figures were made using Adobe Photoshop CS6 version 13.0 (64bit) (Adobe Systems, San Jose, CA).

Graphical Analysis (GA)

GA was used to quantify temporal fluctuations in tissue activity within selected ROIs. For each video, ROIs were manually placed over the most active parts of the tissue – either the hindgut or the *vas deferens* of the male accessory glands. An ROI was selected by clicking a single point on the tissue, around which a square frame was generated. Frame size was adjusted by specifying extensions in the positive and negative x- and y-directions (±x, ±y, preset to 50 px) to include the contracting area while minimizing background interference (step: "Frame Parameters"). Pixel intensity within each ROI was measured automatically frame-by-frame and normalized to the first frame, allowing direct comparison among ROIs and across experimental conditions. GA generates a time-series plot showing pixel-intensity changes on the y-axis (expressed in normalized units, nU) over the duration of the recording on the x-axis (expressed as frame number, corresponding to

time), providing a visual depiction of contraction dynamics. In addition to graph, ROI-specific data were also exported as text files, along with reference images documenting the analyzed regions.

Raw GA data were further processed in Excel (Microsoft, Redmond, WA, USA) and GraphPad Prism 5 (GraphPad Software Inc.). Contraction amplitude was summarized using the interquartile range (Q3–Q1) to reduce the influence of outliers and irregular movement artifacts (Whitley and Ball, 2002). Amplitudes in stimulated tissues were set to 100% to permit normalization across datasets. Progression curves covering the full recording time (3–5 minutes) were generated to represent baseline activity and neuropeptide-induced responses in muscle stimulation or inhibition. All frames were included in the analysis, with no manual removal of irregular segments.

Pixel Activity Analysis (PAA)

PAA was employed to assess overall activity patterns in tissues and whole-organism locomotion. Unlike GA, PAA evaluates every pixel across the full video frame. Pixel activity was defined as intensity changes exceeding a user-defined temporal threshold (t%), which specifies the minimum proportion of frames in which a pixel must vary to be classified as active. It means, higher t% values correspond to lower number of white pixels that indicate increased activity. Unless otherwise noted, t% was set to 80%, enabling suppression of background fluctuations while emphasizing sustained movement.

To reduce computation time for long recordings, an optional frame-skipping parameter (FS) was applied; FS = 0 indicates that every frame was analyzed, while higher values reduce temporal resolution but accelerate processing. PAA outputs a binary PNG image in which active pixels appear white against a black background. In the alternative script version (InsectMotion_ext), active pixels are displayed in red and the background is taken from the first video frame. Both the standard PAA module and the modified InsectMotion_ext implementation were tested, with the latter optimized for visualizing large-scale movements.

Code availability and installation

The InsectMotion code is fully open-source, licensed under the GNU GPLv3 license, and available on GitHub at: https://github.com/medli2568/InsectMotion. The repository contains two script versions: “InsectMotion” and “InsectMotion_ext”, which differ only in the Pixel Activity Analysis (PAA) output. Both scripts can be run directly in a Python Integrated Development Environment (IDE), such as PyCharm, or converted into standalone applications using PyInstaller. PyInstaller packages the Python script into an .exe file in a few simple steps (see “Code Install” section on GitHub for full instructions). This allows users to run the software without requiring a separate Python installation.

RESULTS

We used double IH-staining with CT-DH and MIP antibodies (see Table 2) to map the innervation of both male gonads and hindgut of *B. mori* by CT-DH immunoreactive (IR) neurons. In pharate larvae, PM7–9 neurons of TAG project their axons through proctodaeal nerves (PN, Fig. 1A, B), connect to hindgut in the vicinity of MIP-IR epiproctodeal gland (Fig. 1C, G) and run in parallel to the midgut (Fig. 1D–F). PN protrusions branch on the surface of the hindgut and form numerous secretory varicosities (Fig. 1E). The PN extends beyond the pylorus, where it converges with the principal gastric nerves running along the midgut (Fig. 1F). In pharate adults, we did not detect most of the larval PN, but we detected axons of PM7 in the rectal sack area innervating rectal papillae (Fig. 1G). As previously described (Čižmár et al., 2019), CT-DH- and MIP-IR male specific neurons (MAN9) of TAG innervate male gonads. We summarized the innervation in Fig. 1H–K.

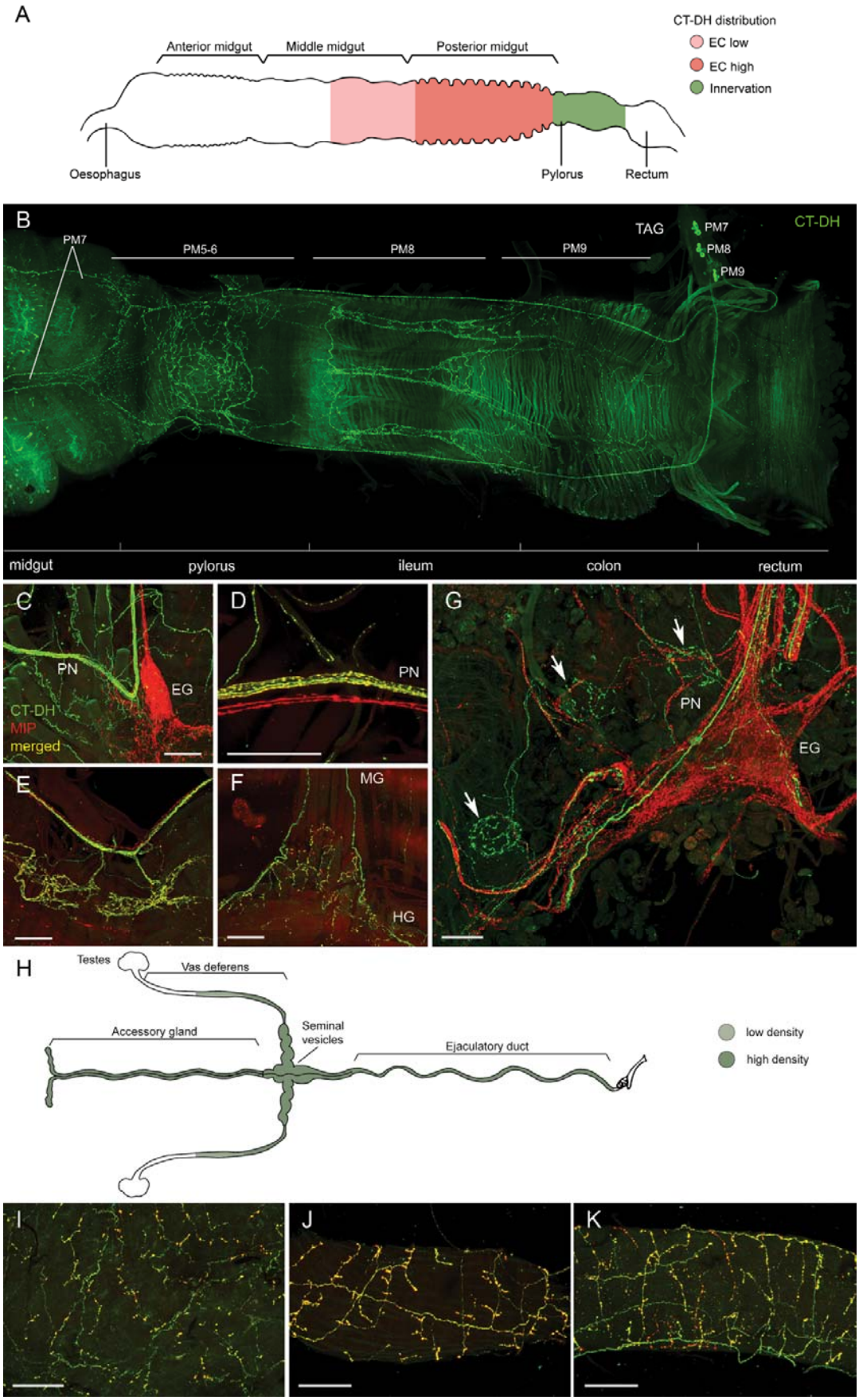
A
CT-DH distribution
EC low
EC high
Innervation
Anterior midgut
Middle midgut
Posterior midgut
Oesophagus
Pylorus
Rectum
B
PM7
PM5-6
PM8
PM9
TAG
PM7
PM8
PM9
CT-DH
midgut
pylorus
ileum
colon
rectum
C
PN
EG
CT-DH
MIP
merged
D
PN
E
F
MG
HG
G
PN
EG
H
Testes
Vas deferens
Accessory gland
Seminal vesicles
Ejaculatory duct
low density
high density
I
J
K

Fig. 1: Innervation of hindgut and male gonads by CT-DH-IR neurons. (A) Distribution of CT-DH-IR endocrine cells (EC; pink), and CT-DH-IR axons (green) in larval gut. (B) Innervation of hindgut and posterior midgut from PM7–PM9 neurons, and pylorus from PM5–6. Double IH staining with CT-DH (green) and MIP (red) antibodies of the gut of pharate larvae (C–F), adult (G), and male gonads (I–K). Proctodeal nerve (PN) innervates gut from the area of MIP-IR epiproctodeal gland (EG) (C). PN axons run in parallel with axons of EG (D). Axons of PM8 and PM9 terminate at the interface of midgut (MG) and hindgut (HG) in E, while PM7 axons continue to the MG (F). In the pharate adult (G), the hindgut region contains only discrete CT-DH-IR innervation, innervation of rectal papillae (arrows), and MIP-IR projections of EG neurons. Innervation of male gonads by MAN9 is summarized in H. Innervation of *vas deferens* (I), accessory glands (J), and ejaculatory duct (K). Scale 100 µm.

To demonstrate the flexibility of InsectMotion for analyzing muscle contractions and locomotor behavior, we visualized the complete workflow used across experiments. The two analytical modules, GA and PAA can be run sequentially on the same recording to obtain both ROI-level contraction profiles and whole-frame activity maps (Fig. 2).

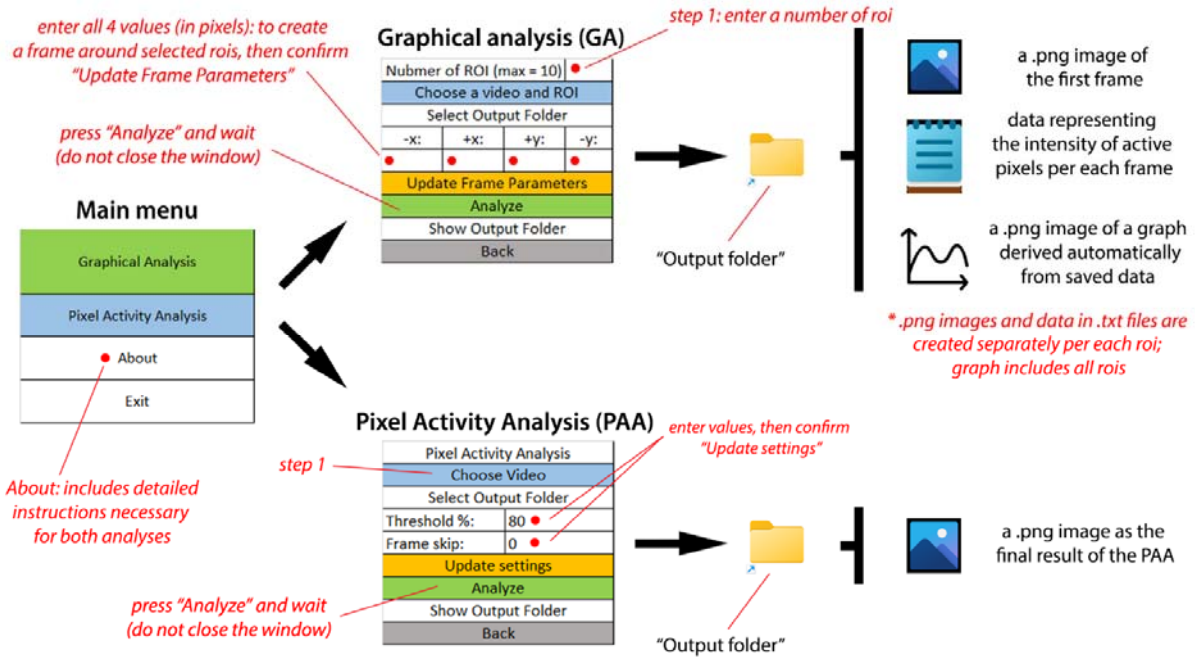

Fig. 2: Schematic representation of InsectMotion workflow. InsectMotion can process video files and provides two distinct analyses: GA and PAA. In GA, the initial step involves entering the number of regions of interest (ROIs). Following this, the process is similar for both analyses: choosing a video file, selecting the output folder, adjusting parameters, confirming the settings and finally starting the analysis. The results are then saved in the designated folders and can be easily accessed directly from the application.

The close association of CT-DH- and MIP-expressing axons with the visceral musculature suggests that these neurons actively control contractile dynamics in both the reproductive tract and hindgut. Guided by these observations, we carried out *in vitro* contraction assays on the larval and adult male hindgut to test neuropeptide-induced muscle activity, adopting a similar approach to that utilized by Čižmár et al. (2019) for male gonoducts. Both larval and adult male hindguts exhibited spontaneous, continuous muscle activity prior to CT34-induced stimulation (Fig. 3D, G), with

average amplitude measured by GA at 40.1% and 31.5%, respectively (Fig. 3A, B). In male reproductive tissues, peristaltic, wave-like muscle activity was observed in control state (Fig. 3J), consistent with previous study (Čižmár et al., 2019), with amplitude measured by GA at 35.3% on average (Fig. 3C). Application of CT34 elicited a significant increase in contraction amplitude across all tissues, with the strongest effect on adult male gonoducts (up to 15-fold) followed by larval hindguts (up to 4.9-fold) and adult male hindguts (up to 4.7-fold). In larval hindguts, these contractions were occasionally accompanied by visible movement of partially digested mulberry leaf material progressing from the midgut toward the rectum, indicating enhanced peristaltic transport in the same region where CT34-induced activity was detected. Additionally, contraction frequency increased in larval and adult male hindguts as displayed in (Fig. 3E, H), whereas male gonoducts showed little changes in frequency (Fig. 3K). Replacing CT34 dilution with 1 µM MIP-1 triggered an immediate inhibitory effect in all tissues. Contraction amplitude and frequency were reduced in larval and adult male hindguts (Fig. 3F, I). Male gonoducts exhibited only baseline muscle activity, reflecting the strongest inhibitory effect (Fig. 3L).

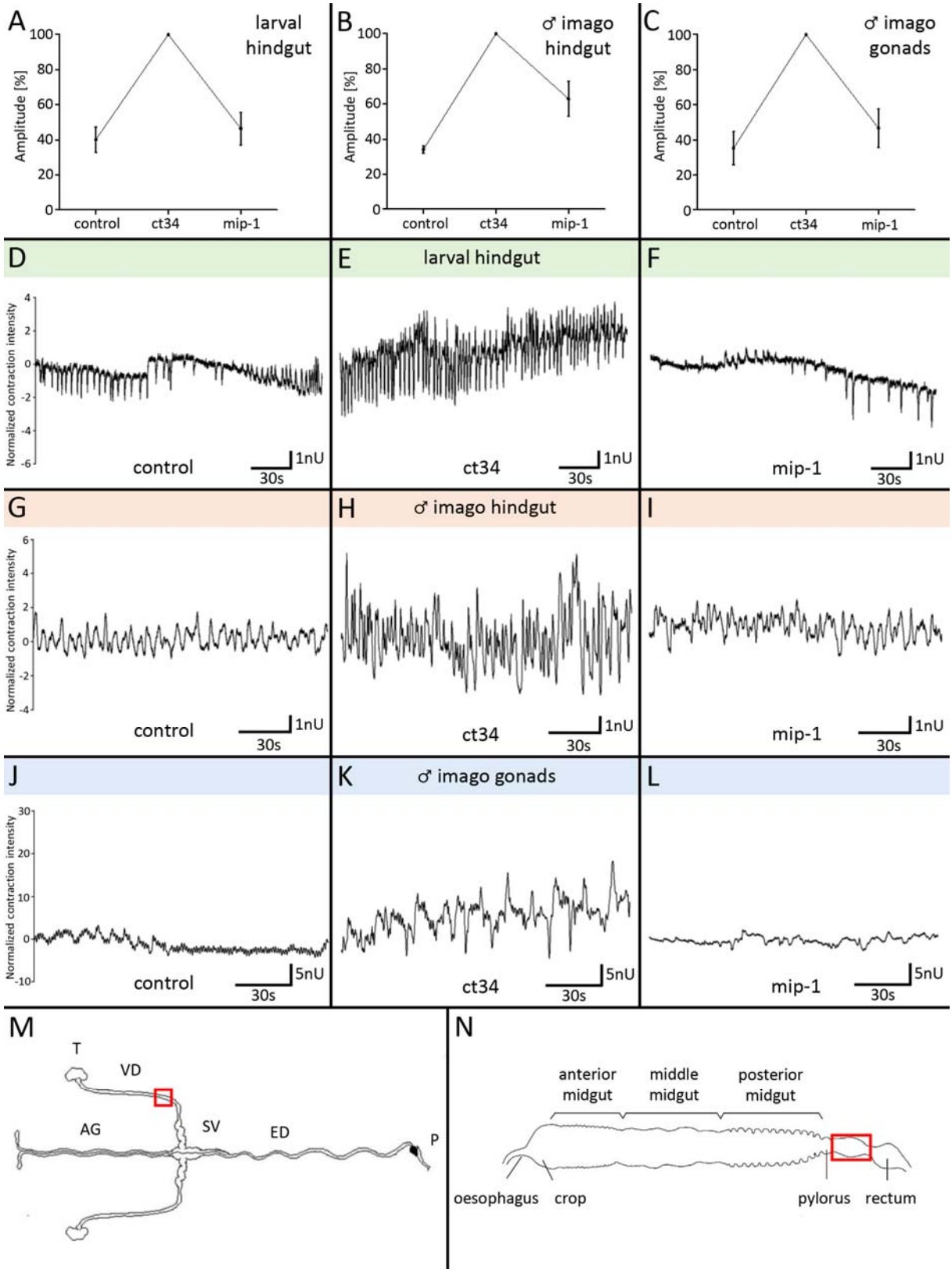

Fig. 3. Quantification of neuropeptide-induced muscle contractions in peripheral organs of *B. mori*, using Graphical Analysis (GA). (A–C) Changes in muscle activity of the hindgut (larvae and adult

males) and adult male reproductive tissues expressed as the percent change in the interquartile range (IQR; Q3-Q1) between control and neuropeptide-treated groups. (D–L) Representative GA outputs showing muscle activity of *B. mori* peripheral organs prior (control) and after application of 1 µM calcitonin 34 (CT34; *I. ricinus*) and 1 µM myoinhibitory peptide 1 (MIP-1; *B. mori*), respectively. (M, N) Schemes of the adult male reproductive system (M) and larval digestive system (N) highlighting the regions with strongest responses to CT34 stimulation. Selected ROIs used for GA are indicated by red squares. Abbreviations: AG – accessory gland; T – *testes*; VD – *vas deferens*; SV – seminal vesicles; ED – ejaculatory duct; P – *penis*.

Trimmed 30-s segments of the same videos used in GA were also analyzed with PAA to visualize neuropeptide-induced changes in muscle activity. Proper adjustment of key PAA parameters, i.e., threshold percentage (t%) and frame skip (FS) was essential for reliably detecting muscle activity.

Both larval (Fig. 4A–D) and adult male hindguts (Fig. 4I–M) exhibited clear differences in the abundance of active regions (white pixels) between control conditions (Fig. 4B, K; suppl. videos 1, 4) and after stimulation with 1 µM CT34 (Fig. 4C, L; suppl. videos 2, 5) or inhibition with 1 µM MIP-1 (Fig. 4D, M; suppl. videos 3, 6). The strongest muscle activity differences was detected in adult male hindgut, as indicated by yellow arrows (Fig. 4J–M). Under control conditions, both larvae (Fig. 4B) and adults (Fig. 4K) showed spontaneous peristaltic movements of the hindgut, which produced a small number of white pixels corresponding to background physiological activity.

In adult male gonoducts (Fig. 4E–H), neuropeptide-induced differences previously detected by GA were less clearly resolved by PAA. Although the stimulated sample showed an increase in activity (Fig. 4G; suppl. video 8), PAA revealed only minimal differences compared with the control (Fig. 4F; suppl. video 7). In contrast, the same recordings showed clear CT34-induced increases in hindgut activity (Fig. 4G, yellow arrow), followed by a marked reduction after MIP-1 application (Fig. 4H; suppl. video 9), consistent with expected neuropeptide effects.

Across all tissues, MIP-1 produced a marked reduction in the number of active pixels (Fig. 5D, H, M) compared to control (Fig. 5B, F, K), reflecting strong myoinhibitory activity.

The modified PAA included in InsectMotion_ext (see the methods) was applied exclusively to *in vivo* locomotion analysis. Using this version, we successfully tracked the movement of a walking male tick on a Petri dish (Fig. 4N; suppl. video 10), demonstrating that PAA can reliably capture large-scale arthropod locomotion.

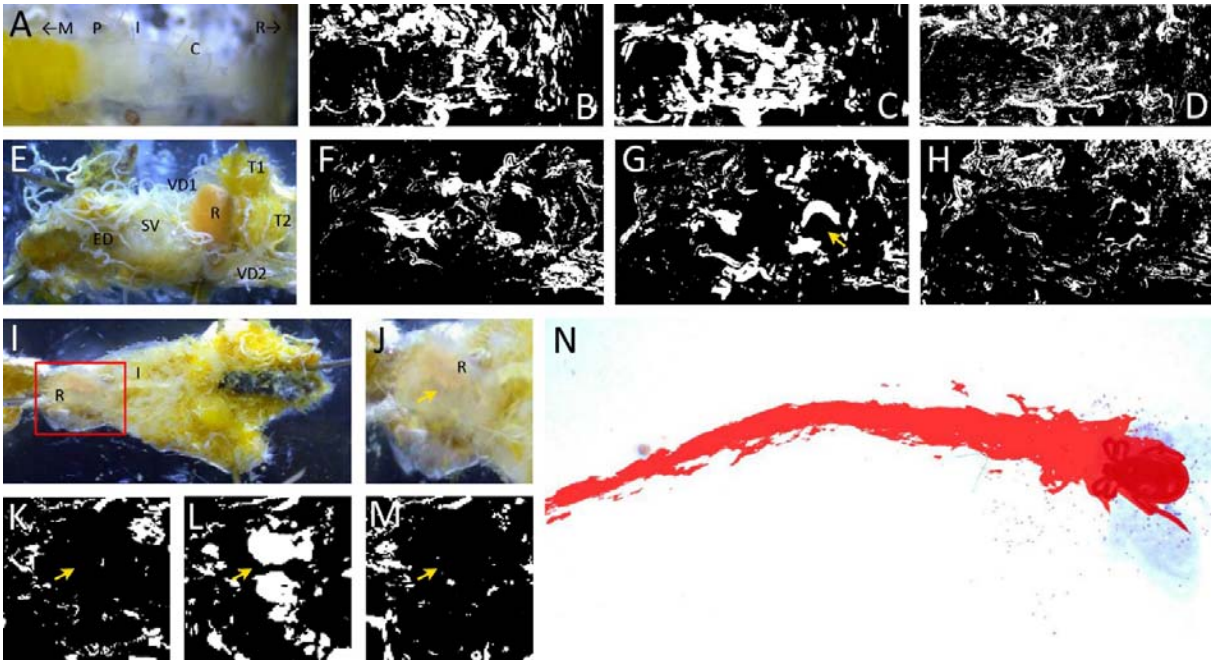

Fig. 4. Detection of organ-specific muscle activity and movements using InsectMotion Pixel Activity Analysis (PAA). (A–D) Visualization of larval hindgut activity under control conditions (B) and after neuropeptide-induced muscle stimulation with 1 µM CT34 (C) or inhibition with 1 µM MIP-1 (D), using parameters: t% = 75; FS = 0. (E–M) Muscle activity in adult male reproductive tissues (E–H) and hindgut (I–M) before (F, K) and after treatment with 1 µM CT34- (G, L) or 1 µM MIP-1 (H, M), using parameters: t% = 85; FS = 0. Original images show anatomy of larval hindgut (A) and adult male reproductive system (E) and hindgut (I; J, detail) with yellow arrows indicating the most active regions. (N) Whole-body movement analysis during male tick locomotion from a trimmed 22 s video, using PAA from the second version of the script (InsectMotion_ext) with parameters: t% = 90, FS = 0. Abbreviations: M – *midgut*; P – *pylorus*; I – *ileum*; C – *colon*; E - ; R – *rectum*; T1/T2 – *testes*; VD1/VD2 – *vas deferens*; SV – seminal vesicles; ED – ejaculatory duct.

DISCUSSION

We developed a new Python-based tool, InsectMotion, to provide a flexible, accessible, and tissue-agnostic platform for quantifying muscle activity and locomotor behavior in insects and other arthropods. The tool was successfully validated both *in vitro* – using contraction assays in *B. mori* tissues, and *in vivo* by tracking the walking behavior of a male tick (*I. ricinus*). Together, these tests demonstrate the broad applicability of the tool across distinct biological contexts. By integrating ROI-based GA with whole-frame PAA, InsectMotion enables precise quantification of contraction dynamics as well as rapid visualization of global movement patterns within the same recording.

Immunohistochemical staining revealed neuropeptidergic innervation in the gonoducts and hindguts, providing a rationale for assessing their functional responses. These stainings were performed using antibodies against insect calcitonin-like diuretic hormone (CT-DH), a peptide family highly conserved across arthropods (Zandawala, 2012). This approach builds on earlier work in *B. mori* characterizing neuropeptide pathways and visceral innervation (Žitňan et al., 1999; 2002; 2007; Bednár et al., 2017; Čižmár et al., 2019; Matsumoto et al., 2019). In line with this anatomical distribution, the homologous calcitonin-like peptide CT34 (*I. ricinus*; Žitňan et al., unpublished data) elicited strong stimulatory effects in all examined tissues, with the most pronounced response

observed in the adult male gonoducts. This observation is consistent with previous results from Čižmár et al. (2019), which demonstrated marked neuropeptide-dependent modulation in male reproductive tissues. Extending the analysis to hindguts, CT34 also enhanced peristaltic activity in male adults and pharate larvae, occasionally promoting visible transport of gut contents toward the rectum. The consistent responsiveness across these tissues supports a broader regulatory role for calcitonin-like peptides in Lepidopteran visceral musculature (LaJeunesse et al., 2010; Coast et al., 2001; Benguettat et al., 2018; Zandawala, 2012; Te Brugge and Schooley, 2008; Čižmár et al., 2019). Conversely, MIP-1 (*B. mori*) consistently induced rapid and pronounced inhibition in all organs tested, reinforcing its conserved myoinhibitory function (Čižmár et al., 2019; Bednar et al., 2017; Kim et al., 2006; 2006). The strong suppression of gonoduct contractility highlights particularly strong sensitivity of reproductive musculature to MIP-1. Likewise, the marked reduction in hindgut contraction amplitude and frequency shows that MIP signaling also modulates visceral motility outside the reproductive system.

The complementary strengths of GA and PAA were evident across experiments. GA reliably quantified amplitude and frequency changes even in narrow, tube-like organs, making it the more sensitive method for detecting subtle neuropeptide effects in the gonoducts. PAA, by contrast, excels at capturing broad changes in spatial movement patterns. It clearly resolved stimulation- and inhibition-induced differences in hindgut preparations, especially in adults where contractions spread across larger tissue regions. However, the same whole-frame approach proved less effective in gonoducts, where contractions involved only a small proportion of pixels. Here, PAA diluted the signal from these localized movements. These insights emphasize that while PAA is powerful for large, spatially dynamic tissues, GA remains necessary for fine-scale or low-amplitude contractions.

The modified PAA implementation in InsectMotion_ext further demonstrated the adaptability of the tool. Its ability to track a walking tick *in vivo* illustrates that the same computational principles can be extended beyond isolated tissues to full-body locomotion in arthropods. This highlights the wider potential of InsectMotion as a general tool for movement analysis across diverse experimental systems.

Overall, this study establishes InsectMotion as a versatile, semi-automated framework suited to both physiological and behavioral analyses. By enabling rapid quantification of neuropeptide-induced muscle responses while also supporting *in vivo* locomotion tracking, the software fills an important methodological gap for researchers working with insects and other invertebrates.

The GitHub repository hosts two versions of the script: “InsectMotion” and “InsectMotion_ext”**,** with the latter serving as an upgraded version of the original. The second version was specifically tested in experiments tracking male tick walking and demonstrated notable improvements. Unlike the original script, which primarily provides black-and-white imaging, “InsectMotion_ext” preserves detailed visual information, including tissue structures, shapes, and colors, which are derived from the first video frame. For example, when studying muscle contractions in specific part of tissue or organs, or movement in particular directions, the ability to observe color variations and structural details provides valuable insights that might be lost in a binary or grayscale representation. As a result, “InsectMotion_ext” script offers greater flexibility and precision, making it especially beneficial for experiments requiring clear differentiation between moving structures and their surroundings.

Several established tools, such as EthoVision XT, DeepLabCut, and ANY-Maze, are widely used for analyzing animal behavior, including tracking, pose estimation, and movement analysis in larger animals. While these programs are powerful and comprehensive, they are often too complex, resource-intensive, and expensive for routine use in arthropod muscle contraction and fine-scale movement studies. For example, EthoVision XT is primarily designed for rodents and small laboratory animals, and DeepLabCut and ANY-Maze, though effective for behavioral assays, lack specialized features tailored to muscle contraction analysis in small arthropod tissues (Bühler et al.,

2023; Mathis et al., 2018; Bailoo et al., 2010). So some experiments need a simpler, more accessible tool specifically optimized for arthropod physiology research.

It is important to note that InsectMotion analyzes the intensity of pixel activity in a single video layer. This means it cannot selectively isolate a tissue or segments at specific depths within the video and all pixels within the selected area are analyzed indiscriminately. Consequently, the output results may be affected by any "contamination" in the video, e.g., shadow, unspecific movement, or anything that will disturb the recording. Despite these limitations, the analysis provides highly precise data. During the examination of muscle dynamics of *B. mori* larval hindgut and adult male gonoducts and hindgut using GA, we observed continuous movement to one side, caused by loosen entomology pins, in which InsectMotion failed to correctly measure the contraction level. Samples must be immobilized tightly on a Petri dish, so GA can truly measure pixel activity change in specific ROIs. These samples were removed to ensure measurement accuracy without compromising overall data integrity.

All video analyses were performed on a computer running on a Windows OS, 13th Gen Intel(R) Core(TM) i7-1355U, 1.70 GHz, 32 GB RAM, 64 bit. Using a computer or laptop with different specifications may negatively impact the analysis process.

InsectMotion stands out due to its user-friendly interface and streamlined software design, which facilitate efficient and intuitive video analysis. Moreover, InsectMotion is freely available on GitHub and exhibits a relatively high sensitivity during measurements. Finally, its customizable parameters using GA and PAA – enhance result accuracy and reliability, making it an accessible and effective tool for arthropod movement studies.

ACKNOWLEDGEMENT

This work was supported by the Slovak grant agencies: APVV-21-0431, APVV-23-0168, VEGA-2/0070/23, and VEGA-2/0037/23.

REFERENCES

Bailoo JD, Bohlen MO, Wahlsten D. The precision of video and photocell tracking systems and the elimination of tracking errors with infrared backlighting. J Neurosci Methods. 2010; 188(1):45–52. doi:10.1016/j.jneumeth.2010.01.035

Bednár B, Roller L, Čižmár D, Mitrová D, Žitňan D. Developmental and sex-specific differences in expression of neuropeptides derived from allatotropin gene in the silkmoth Bombyx mori. Cell Tissue Res. 2017; 368:259–275. doi:10.1007/s00441-016-2556-x

Benguettat O, Jneid R, Soltys J, Loudhaief R, Brun-Barale A, Osman D, Gallet A. The DH31/CGRP enteroendocrine peptide triggers intestinal contractions favoring the elimination of opportunistic bacteria. PLoS Pathog. 2018; 14(9):e1007279. doi:10.1371/journal.ppat.1007279

Bühler D, Power Guerra N, Müller L, Wolkenhauer O, Düffer M, Vollmar B, Kulha A, Wolfien M. Leptin deficiency-caused behavioral change – a comparative analysis using EthoVision and DeepLabCut. Front Neurosci. 2023; 17:1052079. doi:10.3389/fnins.2023.1052079

Čižmár D, Roller L, Pillerová M, Sláma K, Žitňan D. Multiple neuropeptides produced by sex-specific neurons control activity of the male accessory glands and gonoducts in the silkworm Bombyx mori. Sci Rep. 2019; 9:2253. doi:10.1038/s41598-019-38761-x

Coast GM, Webster SG, Schegg KM, Tobe SS, Schooley DA. The Drosophila melanogaster homologue of an insect calcitonin-like diuretic peptide stimulates V-ATPase activity in fruit fly Malpighian tubules. J Exp Biol. 2001; 204(Pt 10):1795–1804. doi:10.1242/jeb.204.10.1795

Daubnerová I, Roller L, Satake H, Zhang C, Kim YJ, Žitňan D. Identification and function of ETH receptor networks in the silkworm Bombyx mori. Sci Rep. 2021; 11:11693. doi:10.1038/s41598-021-91022-8

Hermanson JW, Altenbach JS. Functional anatomy of the primary downstroke muscles in the pallid bat. J Mammal. 1981; 62:795–800. doi:10.2307/1380600

Kim YJ, Žitňan D, Cho KH, Schooley DA, Mizoguchi A, Adams ME. Central peptidergic ensembles associated with organization of an innate behavior. Proc Natl Acad Sci USA. 2006; 103:14211–14216. doi:10.1073/pnas.0603459103

Kim YJ, Žitňan D, Galizia CG, Cho KH, Adams ME. A command chemical triggers an innate behavior by sequential activation of multiple peptidergic ensembles. Curr Biol. 2006; 16(14):1395–1407. doi:10.1016/j.cub.2006.06.027

LaJeunesse DR, Johnson B, Presnell JS, Catignas KK, Zapotoczny G. Peristalsis in the junction region of the Drosophila larval midgut is modulated by DH31 expressing enteroendocrine cells. BMC Physiol. 2010; 10:14. doi:10.1186/1472-6793-10-14

Mathis A, Mamidanna P, Cury KM, Abe T, Murthy VN, Mathis MW, Bethge M. DeepLabCut: markerless pose estimation of user-defined body parts with deep learning. Nat Neurosci. 2018; 21:1281–1289. doi:10.1038/s41593-018-0209-y

Matsumoto S, Kutsuna N, Daubnerová I, Roller L, Žitňan D, Nagasawa H, Nagata S. Enteroendocrine peptides regulate feeding behavior via controlling intestinal contraction of the silkworm Bombyx mori. PLoS One. 2019; 14(7):e0219050. doi:10.1371/journal.pone.0219050

Park D, Veenstra JA, Park JH, Taghert PH. Mapping peptidergic cells in Drosophila: where DIMM fits in. PLoS One. 2008; 3(3):e1896. doi:10.1371/journal.pone.0001896

Pflüger HJ, Duch C. Dynamic neural control of insect muscle metabolism related to motor behavior. Physiology (Bethesda). 2011; 26:293–303. doi:10.1152/physiol.00002.2011

Te Brugge VA, Schooley DA, Orchard I. Amino acid sequence and biological activity of a calcitonin-like diuretic hormone (DH31) from Rhodnius prolixus. J Exp Biol. 2008; 211:382–390. doi:10.1242/jeb.013771

Vassallo M, Pérez-Eid C. Comparative behavior of different life-cycle stages of Ixodes ricinus (Acari: Ixodidae) to human-produced stimuli. J Med Entomol. 2002; 39:234–236. doi:10.1603/0022-2585-39.1.234

Vo-Doan TT, Dung VT, Sato H. A cyborg insect reveals a function of a muscle in free flight. Cyborg Bionic Syst. 2022; 2022:9780504. doi:10.34133/2022/9780504

Whitley E, Ball J. Statistics review 1: presenting and summarising data. Crit Care. 2002; 6:66–71. doi:10.1186/cc1455

Yamanaka N, Hua YJ, Roller L, Spalovská-Valachová I, Mizoguchi A, Kataoka H, Tanaka Y. Bombyx prothoracicostatic peptides activate the sex peptide receptor to regulate ecdysteroid biosynthesis. Proc Natl Acad Sci USA. 2010; 107:2060–2065. doi:10.1073/pnas.0907471107

Yoshida S, Takaki K, Yamawaki Y. Roles of muscle activities in foreleg movements during predatory strike of the mantis. J Insect Physiol. 2023; 145:104474. doi:10.1016/j.jinsphys.2022.104474

Zandawala M. Calcitonin-like diuretic hormones in insects. Insect Biochem Mol Biol. 2012; 42:816–825. doi:10.1016/j.ibmb.2012.06.006

Žitňan D, Hollar L, Spalovská I, Takáč P, Žitňanová I, Gill SS, Adams ME. Molecular cloning and function of ecdysis-triggering hormones in the silkworm Bombyx mori. J Exp Biol. 2002; 205:3459–3473.

Žitňan D, Kim YJ, Žitňanová I, Roller L, Adams ME. Complex steroid-peptide-receptor cascade controls insect ecdysis. Gen Comp Endocrinol. 2007; 153:88–96. doi:10.1016/j.ygcen.2007.04.002

Žitňan D, Ross LS, Žitňanová I, Hermesman JL, Gill SS, Adams ME. Steroid induction of a peptide hormone gene leads to orchestration of a defined behavioral sequence. Neuron. 1999; 23:523–535. doi:10.1016/S0896-6273(00)80805-3

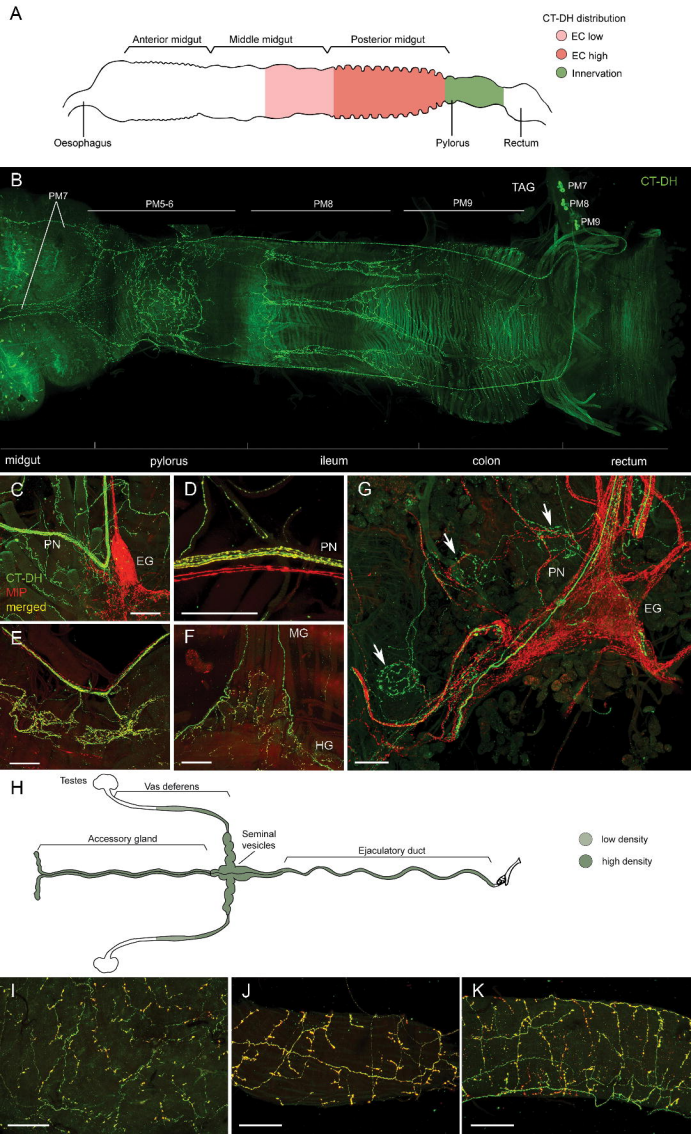
A
Anterior midgut
Middle midgut
Posterior midgut
CT-DH distribution
EC low
EC high
Innervation
Oesophagus
Pylorus
Rectum
B
PM7
PM5-6
PM8
PM9
TAG
PM7
PM8
PM9
CT-DH
midgut
pylorus
ileum
colon
rectum
C
PN
EG
CT-DH
MIP
merged
D
PN
E
F
MG
HG
G
PN
EG
H
Testes
Vas deferens
Accessory gland
Seminal vesicles
Ejaculatory duct
low density
high density
I
J
K

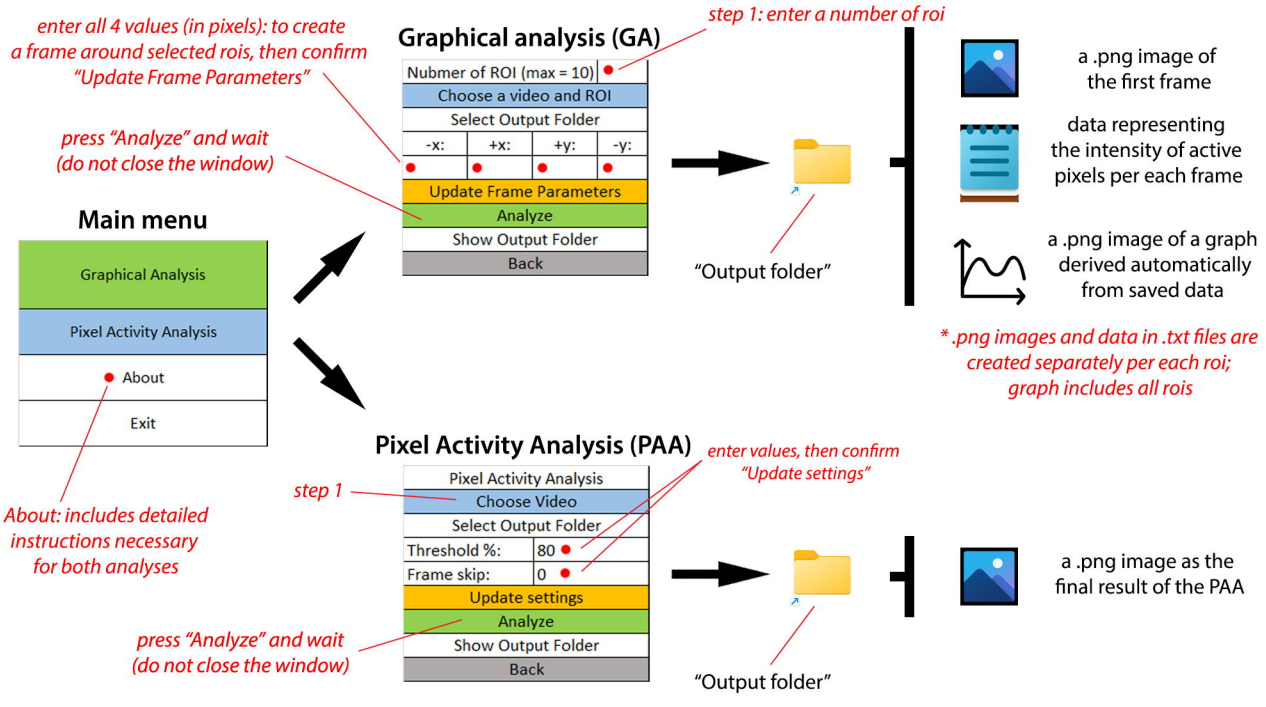
enter all 4 values (in pixels): to create a frame around selected rois, then confirm "Update Frame Parameters"
Graphical analysis (GA)
step 1: enter a number of roi
Nubmer of ROI (max = 10)
Choose a video and ROI
Select Output Folder
-x:
+x:
+y:
-y:
Update Frame Parameters
Analyze
Show Output Folder
Back
press "Analyze" and wait (do not close the window)
Main menu
Graphical Analysis
Pixel Activity Analysis
About
Exit
"Output folder"
a .png image of the first frame
data representing the intensity of active pixels per each frame
a .png image of a graph derived automatically from saved data
* .png images and data in .txt files are created separately per each roi; graph includes all rois
About: includes detailed instructions necessary for both analyses
Pixel Activity Analysis (PAA)
enter values, then confirm "Update settings"
step 1
Pixel Activity Analysis
Choose Video
Select Output Folder
Threshold %:
80
Frame skip:
0
Update settings
Analyze
Show Output Folder
Back
press "Analyze" and wait (do not close the window)
"Output folder"
a .png image as the final result of the PAA

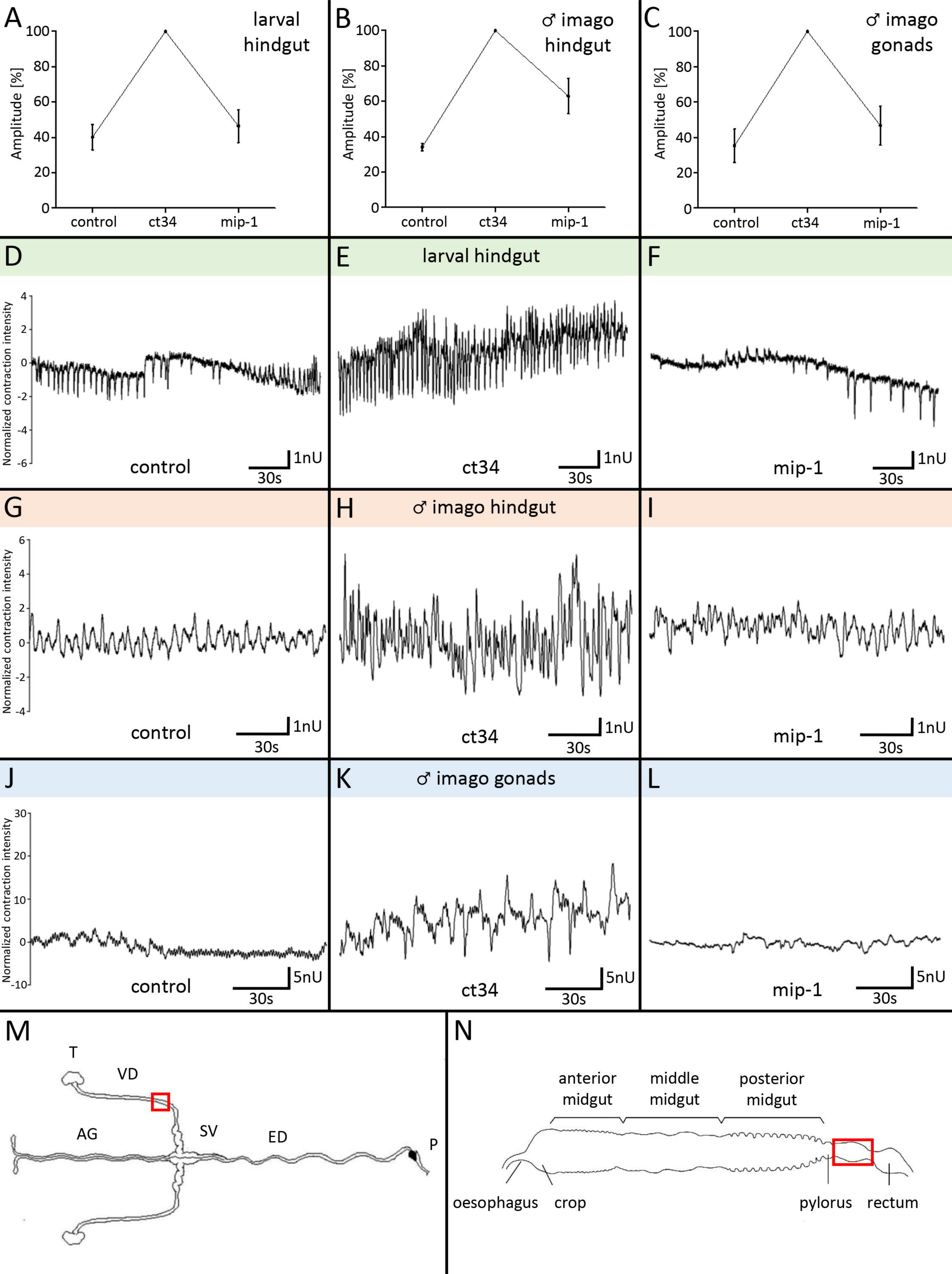
A
larval hindgut
Amplitude [%]
100
80
60
40
20
0
control
ct34
mip-1
B
♂ imago hindgut
C
♂ imago gonads
D
Normalized contraction intensity
4
2
0
-2
-4
-6
control
1nU
30s
E
larval hindgut
ct34
F
mip-1
G
6
4
2
0
-2
-4
H
♂ imago hindgut
I
J
30
20
10
0
-10
5nU
K
♂ imago gonads
L
M
T
VD
AG
SV
ED
P
N
anterior midgut
middle midgut
posterior midgut
oesophagus
crop
pylorus
rectum

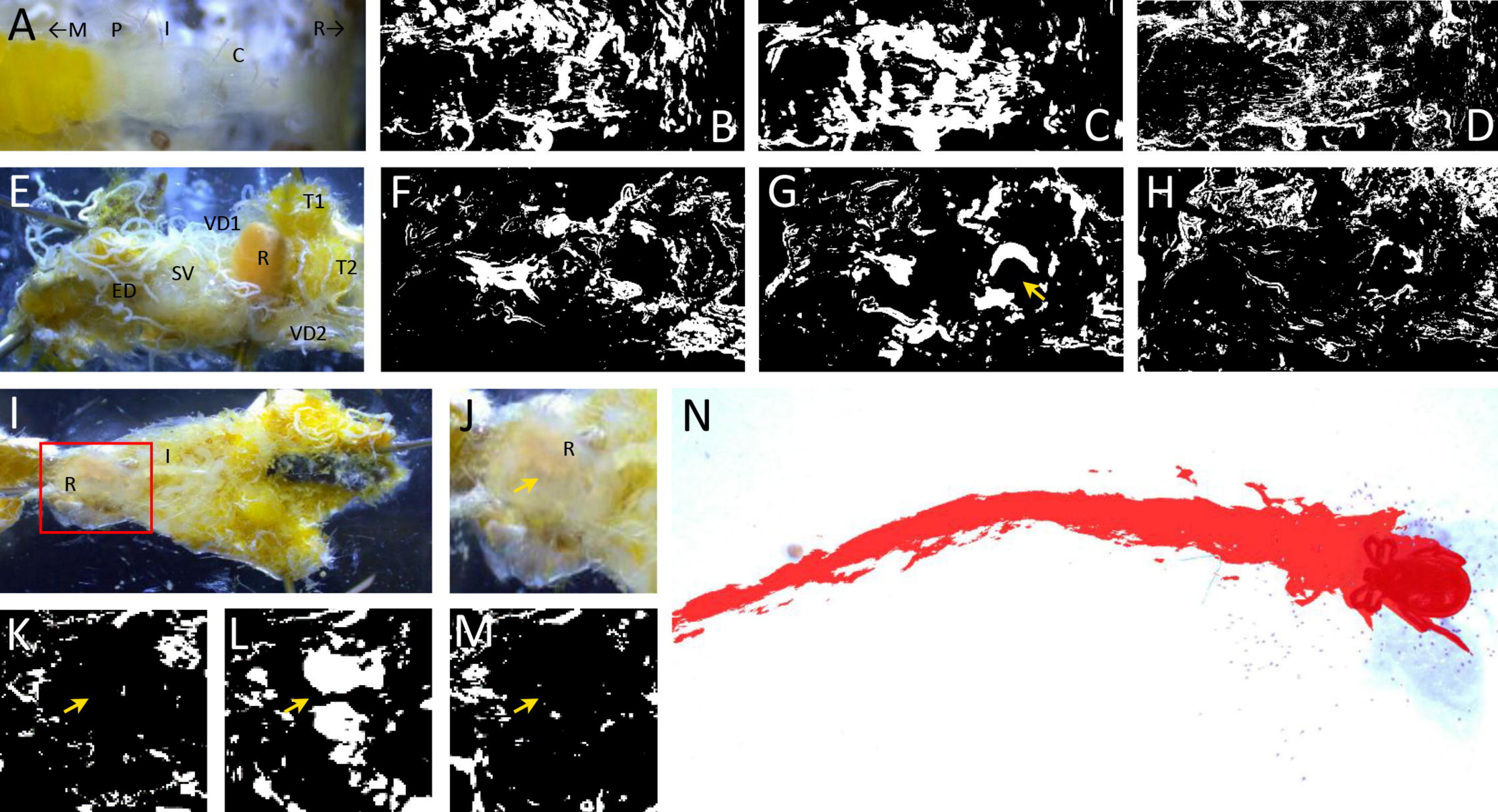
A
←M
P
I
C
R→
B
C
D
E
T1
VD1
R
T2
SV
ED
VD2
F
G
H
I
R
I
J
R
N
K
L
M